Journal of the Serbian Chemical Society
JSCS@tmf.bg.ac.rs • www.shd.org.rs/JSCS
J. Serb. Chem. Soc. 90 (7–8) 837–856 (2025)
JSCS–5424
Original scientific paper
Published 12 August, 2025

Comparative *in silico*/*in vitro* analysis of pharmacokinetic profiles of BET inhibitors

MLADEN KORAVOVIĆ[1]*, MILENA KOVAČEVIĆ[2]**, MARIJA JOVANOVIĆ[2], GORDANA TASIĆ[1], ANAND MAYASUNDARI[3], GISELE NISHIGUCHI[3], BOJAN MARKOVIĆ[4], ZORAN RANKOVIĆ[3,5] and VLADIMIR SAVIĆ[1]

[1]Department of Organic Chemistry, University of Belgrade – Faculty of Pharmacy, Vojvode Stepe 450, 11221 Belgrade, Serbia, [2]Department of Pharmacokinetics and Clinical Pharmacy, University of Belgrade – Faculty of Pharmacy, Vojvode Stepe 450, 11221 Belgrade, Serbia, [3]Department of Chemical Biology and Therapeutics, St. Jude Children's Research Hospital, 262 Danny Thomas Place, Memphis, TN, 38105, USA, [4]Department of Pharmaceutical Chemistry, University of Belgrade – Faculty of Pharmacy, Vojvode Stepe 450, 11221 Belgrade, Serbia and [5]Centre for Protein Degradation, Institute of Cancer Research, 15 Cotswold Road, Sutton, London, SM2 5NG, UK

(Received 11 December 2024, revised 18 May, accepted 15 June 2025)

Abstract: Pharmacokinetic limitations are a common cause of drug development failure, making early-stage profiling essential to mitigate financial risks and guide compound optimization. The computational tools capable of predicting pharmacokinetic properties offer a valuable resource for the prioritizing of candidates during early discovery phases. This study provides a comparative analysis of *in silico* and *in vitro* pharmacokinetic profiles of bromodomain and extraterminal domain (BET) inhibitors (BIs), focusing on sixteen (+)-JQ1--derived compounds we previously synthesized. Using ADMETlab 2.0 software, we predicted key absorption, distribution, metabolism, and excretion (ADME) parameters and compared them with experimentally determined data. Strong correlations were observed for plasma protein binding, whereas notable discrepancies were identified in permeability and clearance values. Additionally, the analysis underscores the role of CYP3A4 as a critical enzyme in the metabolism of several BIs. These findings demonstrate the utility of computational tools like ADMETlab 2.0 for early pharmacokinetic profiling while highlighting the need for validation and refinement of predictive models. This work provides valuable insights into the pharmacokinetics of BIs and supports the integration of computational and experimental approaches in drug discovery.

Keywords: (+)-JQ1; ADME analysis; ADMETlab 2.0; drug development.

*,** Corresponding authors. E-mail: (*)mladen.koravovic@pharmacy.bg.ac.rs; (**)milena.kovacevic@pharmacy.bg.ac.rs
https://doi.org/10.2298/JSC241211042K

INTRODUCTION

The challenges related to pharmacokinetics frequently contribute to the failure of drug development, emphasizing the importance of early evaluation and refinement of these properties during drug discovery. In the context of drug development, particularly for orally administered agents like bromodomain and extra-terminal domain (BET) inhibitors, the desirable pharmacokinetic properties include: high intestinal absorption and permeability to ensure sufficient bioavailability; moderate to high metabolic stability to avoid rapid degradation; balanced plasma protein binding to ensure the adequate free (unbound) drug concentration and avoid the potential variability related to the albumin concentration; optimal volume of distribution, indicating the ability to reach the target tissues, including those with poor blood supply; reasonable half-life to maintain the therapeutic plasma levels without frequent dosing; and the low potential for drug-drug interactions, especially via cytochrome P450 (CYP450) enzymes like CYP3A4. For BET inhibitors (BIs) targeting systemic or central nervous system (CNS) malignancies, additional desirable features include blood–brain barrier (BBB) penetration and resistance to P-glycoprotein (P-gp)-mediated efflux, which can hinder CNS drug delivery. These criteria guide early-stage screening to prioritize candidates likely to exhibit effective and safe pharmacological profiles *in vivo*.

The computational tools, such as ADMETlab 2.0, enable the prediction of absorption, distribution, metabolism, excretion, and toxicity (ADMET) properties, offering valuable insights for drug design.[1] Building on our previous research,[2] this study evaluates the pharmacokinetics of (+)-JQ1-derived, BIs using a combination of *in silico* and *in vitro* approaches.

The BET protein family, comprising BRD2, BRD3, BRD4 and BRDT, plays a crucial role in transcriptional regulation by recognizing the acetylated lysine residues on chromatin.[3–5] These proteins are implicated in various diseases, making them attractive therapeutic targets. BIs have shown efficacy in hematological malignancies such as acute myeloid leukemia,[7] multiple myeloma[8] and diffuse large B-cell lymphoma,[9] as well as in solid tumors including triple-negative breast cancer,[10] glioblastoma[11] and NUT midline carcinoma.[12] Beyond oncology, BET inhibition is being explored in inflammatory and autoimmune disorders such as systemic lupus erythematosus[13] and rheumatoid arthritis[14] and even in fibrotic diseases[15] and cardiovascular conditions.[16] The wide range of potential indications highlights the clinical relevance of pharmacokinetically optimizing BIs for both systemic and tissue-targeted therapies. Among the BIs, (+)-JQ1 has shown remarkable preclinical efficacy across numerous disease models.[17] However, its limited pharmacokinetic properties have posed challenges for clinical application.[18]

To address these limitations, our group has developed a series of potent (+)--JQ1-derived amides.[2] Expanding on this work, we utilized ADMETlab 2.0 to predict the pharmacokinetic profiles of these novel compounds and compared the

computational predictions with experimental data to identify correlations. These findings enhance the understanding of Bis' pharmacokinetics, facilitating the development of next-generation BIs and enabling the selection of promising candidates for further evaluation. This study systematically correlates *in silico* and *in vitro* ADME results for BIs, offering a comprehensive pharmacokinetic discussion that integrates computational predictions with experimental findings.

The chemical structures of the studied BIs are presented in Fig. 1.

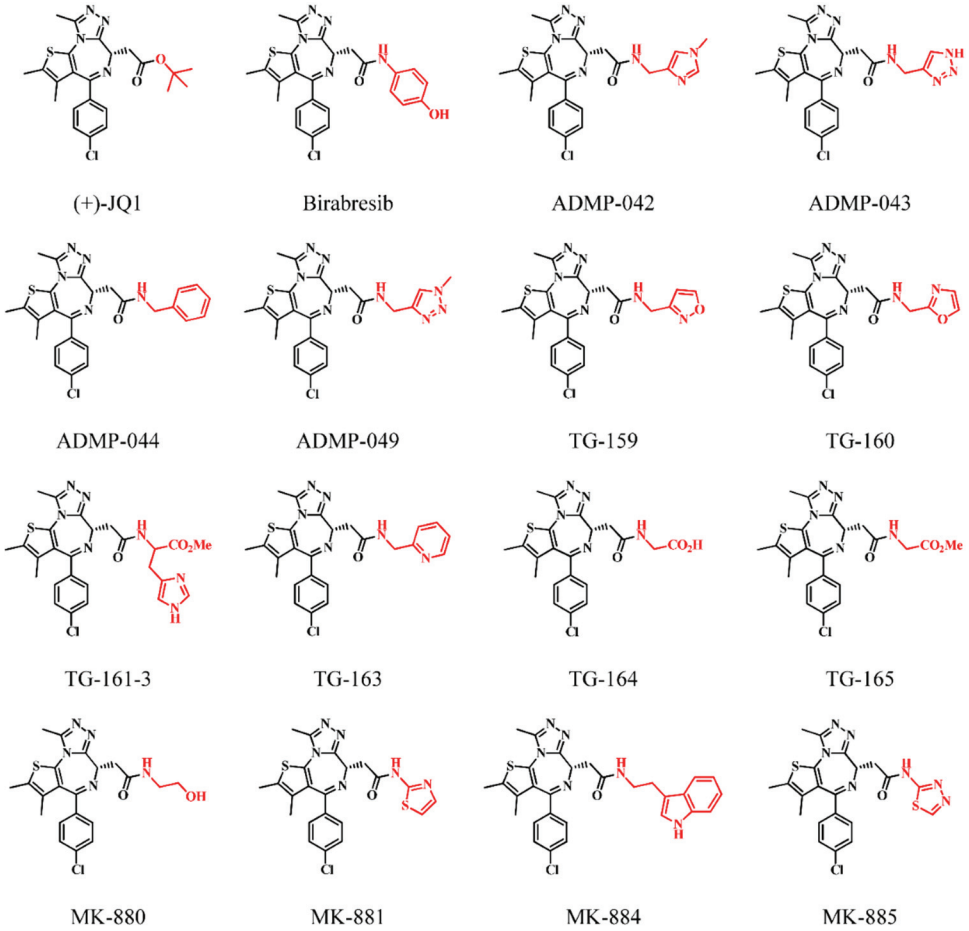

Fig. 1. Chemical structures of the studied (+)-JQ1-derived BIs (parts of molecules marked in red indicate structural differences among the studied BIs).

MATERIALS AND METHODS

In this study, ADMETlab 2.0 was used to predict the ADMET properties of previously characterized BIs *in vitro*.[2] This platform utilizes a comprehensive ADMET database for predicting various pharmacokinetic and toxicological parameters using QSAR models built from

288,967 chemicals.[1,19] The predictions are based on six modelling algorithms: random forests (RF), support vector machine (SVM), recursive partitioning regression (RP), partial least square (PLS), naive Bayes (NB) and decision tree (DT).[1] ADMETlab 2.0 includes 17 physicochemical properties, 13 medicinal chemistry properties, 23 ADME properties, 27 toxicity endpoints and 8 toxicophore rules (751 substructures).[20] The structures of BIs were drawn using ChemDraw Ultra 12.0, with SMILES input and output retrieved as .csv files. ADMETlab 2.0 was chosen for its accuracy and large database,[1,20] providing the comprehensive pharmacokinetic predictions that align with the study's needs.

Additionally, MarvinSketch 4.1.13 was used to predict ionization and logD values. Statistical analysis was performed using IBM SPSS Statistics 28.0. The strength and the direction of association between ADMETlab 2.0 output and experimental data were evaluated using bivariate Spearman's correlation, with Spearman's rank correlation coefficients (ρ) and p values reported. Correlation interpretation followed these criteria: $\rho \geq 0.700$ (strong), $0.400 \leq \rho < 0.700$ (moderate) and $\rho < 0.400$ (weak).[21] The correlations were also assessed using the Wilcoxon signed-rank test, and the results were visualized with box-and-whisker plots. Pharmacokinetic parameters were represented by median values and interquartile ranges (*IQR*s).

A sample of sixteen compounds was selected to balance dataset robustness with detailed analysis. This structurally diverse set allows evaluation of pharmacokinetic properties and their relationship to structural variation. The focused nature of the study provides detailed data for further research.

To ensure the clarity and the consistency throughout this study, we introduce a specific notation: results obtained through computational predictions, referred to as *in silico*, are denoted with the superscript "IS" (*e.g.*, predicted pharmacokinetic parameter^{IS}). Similarly, the results derived from experimental assays, referred to as *in vitro*, are denoted with the superscript "IV" (*e.g.*, measured pharmacokinetic parameter^{IV}). This notation is applied consistently throughout the text to provide a clear and immediate distinction between the two types of datasets. However, in tables where the data are already explicitly classified into *in silico* and *in vitro* groups, the superscripts "IS" and "IV" are omitted to maintain visual simplicity.

RESULTS AND DISCUSSION

Absorption

A total of seven pharmacokinetic parameters relevant for absorption were predicted using ADMETlab 2.0: three parameters predicting the extent of absorption – *HIA prob.*^{IS}, *F(20%)*^{IS} and *F(30%)*^{IS}, two parameters predicting the permeability – *Caco-2 perm.*^{IS} and *MDCK perm.*^{IS}, and two parameters predicting whether the studied BIs act as P-gp substrates or inhibitors – *P-gp sub.*^{IS} and *P-gp inh.*^{IS}, respectively. The obtained *in silico* and *in vitro* results regarding absorption are presented in Tables I and II.

Heatmap is based on an *in silico* empirical decision. The cells marked in green, yellow or red denote excellent, medium or poor results, respectively.[22]

The extent of the human intestinal absorption (*HIA*) was reported through the probabilities (*HIA prob.*^{IS} values) of the tested compounds to have *HIA* below 30 %. Hence, the lower the *HIA prob.*^{IS}, the higher the intestinal absorption. These probabilities ranged from 0.004 to 0.047. Thirteen out of sixteen tested candidates had *HIA prob.*^{IS} below 0.010, appropriate for orally administered drugs. The

compound MK-881 showed the best *HIA prob.*^{IS} of 0.004, similar to birabresib as the reference drug. Interestingly, the lowest value of intestinal absorption was predicted for (+)-JQ1, whose *HIA prob.*^{IS} was as high as 0.047.

TABLE I. Absorption-related *in silico* results

Compound	*HIA prob.*[a]	*F(20%)*[b]	*F(30%)*[c]	*Caco-2 perm.*[d]	*Caco-2 perm. calc.*, nm s^{-1}	*MDCK perm.*[e], nm s^{-1}	*P-gp sub.*[f]	*P-gp inh.*[g]
(+)-JQ1	0.047	0.002	0.022	–4.475	334.97	215.99	0.006	0.001
Birabresib	0.004	0.001	0.001	–4.787	163.31	187.98	0.714	0.001
ADMP-042	0.007	0.001	0.218	–4.656	220.80	268.83	0.812	0
ADMP-043	0.007	0.001	0.002	–4.826	149.28	171.63	0.992	0
ADMP-044	0.005	0.001	0.001	–4.703	198.15	182.99	0.033	0.002
ADMP-049	0.018	0.002	0.009	–4.590	257.04	263.26	0.860	0
TG-159	0.007	0.001	0.001	–4.616	242.10	195.39	0.243	0
TG-160	0.006	0.001	0.001	–4.615	242.66	259.52	0.129	0
TG-161-3	0.006	0.001	0.003	–4.718	191.43	171.08	0.989	0
TG-163	0.005	0.001	0.001	–4.672	212.81	235.96	0.043	0.001
TG-164	0.008	0.001	0.001	–4.793	161.06	246.16	0.685	0.001
TG-165	0.014	0.002	0.004	–4.587	258.82	255.60	0.606	0.001
MK-880	0.005	0.002	0.002	–4.512	307.61	276.85	0.730	0
MK-881	0.004	0.001	0.002	–4.696	201.37	253.39	0.285	0
MK-884	0.006	0.001	0.009	–5.026	94.19	164.93	0.430	0.034
MK-885	0.005	0.001	0.002	–4.712	194.09	277.64	0.936	0

[a]The output values, ranging between 0 and 1, represent the probability that the compound has human intestinal absorption < 30 %. [b]The output values, ranging between 0 and 1, represent the probability that the compound has bioavailability < 20 %. [c]The output values, ranging between 0 and 1, represent the probability that the compound has bioavailability < 30 %. [d]Optimal is > –5.15. [e]Low permeability: < 20 nm s^{-1}; medium permeability: 20–200 nm s^{-1}; high permeability: > 200 nm s^{-1}. [f]The output values, ranging between 0 and 1, represent the probability that the compound is a P-glycoprotein substrate. [g]The output values, ranging between 0 and 1, represent the probability that the compound is a P-glycoprotein inhibitor

The last two parameters used to predict the extent of absorption were *F(20%)*^{IS} – the probability of a drug having oral bioavailability below 20 % and *F(30%)*^{IS} – the probability of a drug having oral bioavailability below 30 %. As for the previous parameter, lower probability values denote higher oral bioavailability. The range of *F(20%)*^{IS} values (0.001–0.002) was narrow, thus not particularly informative for comparing the compounds, although it did suggest that the studied compounds have very low probabilities of exhibiting bioavailabilities below 20 %. In contrast to *F(20%)*^{IS}, *F(30%)*^{IS} highlighted ADMP-042 as the compound with the highest predicted value, indicating the greatest probability of having bioavailability below 30 % among the studied BIs. The extent of the human intestinal absorption (HIA) was reported through the probabilities (*HIA prob.*^{IS} values) of the tested compounds to have HIA below 30 %. Hence, the lower the *HIA prob.*^{IS}, the higher the intestinal absorption. These probabilities ranged from 0.004 to 0.047. Thirteen out of sixteen tested candidates had *HIA prob.*^{IS} below 0.010,

appropriate for orally administered drugs. The compound MK-881 showed the best *HIA prob.*^{IS} of 0.004, similar to birabresib as the reference drug. Interestingly, the lowest value of intestinal absorption was predicted for (+)-JQ1, whose *HIA prob.*^{IS} was as high as 0.047.

TABLE II. *In vitro* permeability data from PAMPA and Caco-2 assay; Avg. *P* – average permeability; Avg. P_{app} *A–B* – average apparent permeability coefficient from apical to basolateral side; Avg. P_{app} *B–A* – average apparent permeability coefficient from basolateral to apical side; *ER* – efflux ratio; *R* – recovery; *SD* – standard deviation

Compound	PAMPA		Caco-2 permeability assay		
	Avg. *P*±*SD*, 10^{-6} cm s^{-1}	*R*±*SD* / %	Avg. P_{app} A–B±*SD* nm s^{-1}	Avg. P_{app} B–A±*SD*, nm s^{-1}	*ER*
(+)-JQ1	> 1800	59.52±16.79	63.97±11.63	46.67±12.91	0.73
Birabresib	315.13±23.20	95.20 ±1.42	221.60±67.35	485.39±142.68	2.19
ADMP-042	0	44.20±6.33	9.16±0.39	311.21±92.63	33.96
ADMP-043	2.09±0.68	23.68±1.17	2.50±0.41	28.03±8.54	11.20
ADMP-044	1797.07±277.74	71.66±11.23	42.20±14.58	44.51±13.17	1.05
ADMP-049	14.04±3.37	32.25±2.47	6.17±3.15	246.45±133.88	39.93
TG-159	274.52±41.45	65.06±1.82	150.34±40.42	777.89±185.65	5.17
TG-160	97.17±7.28	61.69±1.68	30.39±7.46	297.37±55.89	9.79
TG-161-3	0	33.64±0.78	7.74±10.38	14.18±5.75	1.83
TG-163	177.45±20.63	74.32±3.59	98.37±9.55	568.43±106.65	5.78
TG-164	0.54±0.93	8.52±0.26	4.51±0.95	7.81±5.20	1.73
TG-165	231.31±53.54	47.45±5.58	63.76±8.53	307.31±35.59	4.82
MK-880	20.80±1.19	31.11±1.22	6.98±0.95	83.32±15.08	11.94
MK-881	544.83±34.50	80.49±1.47	19.10±12.38	41.09±8.55	2.15
MK-884	>1800	90.51±N/D	5.69±1.43	13.79±7.81	2.42
MK-885	533.96±237.40	91.83±4.43	66.46±26.53	180.11±54.68	2.71

The predicted Caco-2 permeability was reported through *Caco-2 perm.*^{IS} with a subsequent calculation to derive *Caco-2 perm. calc.*^{IS}. All candidates showed an acceptable *Caco-2 perm.*^{IS} since all values were greater than –5.15. The compound MK-884 showed the poorest *Caco-2 perm.*^{IS}, followed by ADMP-043 and TG--164, whereas (+)-JQ1 showed the best *Caco-2 perm.*^{IS} The set of *in silico*- (*Caco-2 perm. calc.*^{IS}, Table I) and *in vitro*-obtained results (Avg. P_{app} A–B^{IV}, Table II) regarding Caco-2 permeability were compared through the Wilcoxon signed--ranked test (Fig. S-1A of the Supplementary material to this paper). The median value regarding predicted Caco-2 permeability notably surpassed that determined through *in vitro* assessment with the respective values of 207.09 nm s^{-1} (*IQR* 170.34–253.44 nm s^{-1}) and 24.74 nm s^{-1} (*IQR* 6.37–65.84 nm s^{-1}). Thus, the direct comparison between *in silico*- and *in vitro*-obtained Caco-2 permeability results demonstrated a statistically significant difference ($p < 0.001$). A bar plot with paired data (Fig. S-1B of the Supplementary material) provides a visual representation that more effectively highlights the relationship between *in silico* and *in*

vitro results, offering a clearer perspective on their degree of alignment. In general, all BIs exhibited higher predicted Caco-2 permeabilities compared to those determined *in vitro*.

MDCK permeability was predicted as well and reported through *MDCK perm.*^{IS}. Based on this parameter, the studied compounds were classified as medium (0.2×10^{-5}–2×10^{-5} cm s^{-1}) or high permeable (above 2×10^{-5} cm s^{-1}). Ten candidates, including (+)-JQ1, had high, whereas six candidates, including birabresib, had medium predicted MDCK permeabilities.

The final two predicted parameters, *P-gp sub.*^{IS} and *P-gp inh.*^{IS}, keep to absorption and predict whether the tested BIs perform as substrates or inhibitors of P-gp, respectively. Tested compounds differed significantly in terms of being P-gp substrates, having *P-gp sub.*^{IS} values from 0.006 to 0.989. This variability might affect drug distribution and therefore requires attention. The highest probability of being a P-gp inhibitor was predicted for MK-884, with *P-gp inh.*^{IS} of 0.034. In contrast, other candidates showed substantially lower *P-gp inh.*^{IS} comparable to birabresib or (+)-JQ1. Interestingly, nine candidates had *P-gp inh.*^{IS} equal to zero.

In vitro assessment of absorption of the studied BIs was performed *via* PAMPA and Caco-2 permeability assay.[2] A notable dispersion of results was observed, signifying substantial variability in permeabilities of the tested compounds. PAMPA reported the highest permeability for ADMP-044, approximately six times higher than for birabresib. Also, high permeabilities were observed for MK-881 and MK-885, followed by birabresib. Only four compounds (MK-881, MK-884, MK-885 and birabresib) had recovery (*R*) above 80 %.

Table S-I of the Supplementary material provides a detailed overview of the statistical correlations between *in silico*- and *in vitro*-assessed pharmacokinetic parameters relevant to absorption. Moderate negative correlations were noted between *HIA prob.*^{IS} and PAMPA results, *P-gp sub.*^{IS} and Avg. P^{IV}, and *P-gp inh.*^{IS} and ER^{IV}.

Distribution

The pharmacokinetic parameters relevant for distribution include BBB penetrability (*BBB pen.*^{IS}), plasma protein binding (PPB^{IS} and PPB^{IV}), volume of distribution ($V_d{}^{IS}$) and unbound fraction ($F_u{}^{IS}$). The results obtained from ADMETlab 2.0 and *in vitro* assessments are presented in Table III.

The predicted BBB penetrability showed high values ranging from 0.808 to 0.992, with birabresib having a probability of 0.923. The lowest *BBB pen.*^{IS} was estimated for compound TG-164, likely due to its higher hydrophilicity resulting from the presence of a free carboxylic acid. Despite the high values being marked in red according to the ADMETlab 2.0's empirical decision, BBB penetrable BIs are generally desirable for certain CNS diseases.[23]

TABLE III. Representation of *in silico*- and *in vitro*-obtained results regarding distribution; Heatmap is based on an *in silico* empirical decision. Cells marked in green or red denote excellent or poor results, respectively;[22] V_d – volume of distribution; F_u – unbound fraction; *SD* – standard deviation

Compound	*In silico*-obtained results				*In vitro*-obtained results
	BBB pen.[a]	*PPB*[b], %	V_d[c] / L kg^{-1}	F_u[d] / %	*PPB*±*SD*, %
(+)-JQ1	0.987	93.97	1.419	9.76	99.15±0.03
Birabresib	0.923	96.10	1.17	5.97	97.27±0.15
ADMP-042	0.904	82.36	1.674	26.74	98.53±0.40
ADMP-043	0.940	91.87	1.683	13.73	94.77±0.32
ADMP-044	0.991	94.89	0.933	11.07	98.68±0.14
ADMP-049	0.931	91.08	1.686	20.18	97.54±0.04
TG-159	0.971	93.59	1.239	11.02	93.45±0.45
TG-160	0.981	86.44	1.030	23.21	94.08±0.57
TG-161-3	0.937	77.41	1.105	28.23	92.68±0.71
TG-163	0.984	90.26	1.238	17.14	97.21±0.24
TG-164	0.808	85.37	0.876	15.73	85.57±2.50
TG-165	0.992	86.02	1.478	22.58	91.03±1.46
MK-880	0.985	79.77	1.607	24.88	86.90±0.67
MK-881	0.985	91.96	1.136	11.16	98.24±0.14
MK-884	0.983	95.93	1.210	6.92	99.59±0.03
MK-885	0.983	93.57	1.248	7.87	97.22±0.37

[a]The output values, ranging between 0 and 1, represent the probability that the compound is blood-brain barrier penetrable. [b]Optimal is ≤90 %. [c]Optimal is from 0.04 to 20 L kg^{-1}. [d]Low is <5 %, medium is 5–20 % and high is >20 %

The *in vitro* experiments revealed higher affinities for 14 out of 16 tested compounds compared to *in silico* predictions. The Wilcoxon signed-rank test (Fig. S-2A of the Supplementary material) showed a statistically significant difference ($p < 0.001$) between PPB^{IS} and PPB^{IV}, with median values of 91.47 % (*IQR* 85.69––93.78 %) and 97.21 % (*IQR* 92.87–98.46 %), respectively. A bar plot with paired data (Fig. S-2B of the Supplementary material) visually depicts the relationship between *in silico* and *in vitro* results, providing a more intuitive understanding of their degree of alignment.

The V_d^{IS} ranged between 0.876 and 1.686 L kg^{-1}, with TG-164 predicted to have the lowest V_d^{IS}. ADMP-049 demonstrated the highest V_d^{IS}, despite not being classified among the most lipophilic compounds.

Table S-I provides a comprehensive representation of the statistical correlations between *in silico*- and *in vitro*-assessed pharmacokinetic parameters relevant to distribution. Moderate positive correlation was observed between $BBB\ pen.^{IS}$ and Avg. P^{IV}. Additionally, PPB^{IS} exhibited strong positive correlations with both Avg. P^{IV} and R^{IV}. Moderate positive correlations were also found between *in silico*- and *in vitro*-assessed plasma protein binding values, as well as

between V_d^{IS} and ER^{IV}. Notably, a strong negative correlation was identified between F_u^{IS} and Avg. P^{IV}, while F_u^{IS} and R^{IV} demonstrated a moderate negative correlation.

Metabolism and excretion

In silico evaluation of metabolism included predicting the probabilities of the BIs being substrates or inhibitors of CYP1A2, CYP2C9, CYP2C19, CYP2D6 and CYP3A4. Results are shown in Table IV.

TABLE IV. Probabilities of the studied bis being cyp450 substrates and/or inhibitors; the output values, ranging between 0 and 1, represent the probability that the compound is cytochrome P450 substrate and/or inhibitor

Compound	CYP1A2		CYP2C9		CYP2C19		CYP2D6		CYP3A4	
	Sub.	Inh.	Sub.	Inh.	Sub.	Inh.	Sub.	Inh.	Sub.	Inh.
(+)-JQ1	0.943	0.098	0.115	0.837	0.909	0.635	0.019	0.040	0.959	0.458
Birabresib	0.952	0.173	0.728	0.890	0.744	0.495	0.078	0.399	0.960	0.665
ADMP-042	0.933	0.170	0.057	0.371	0.748	0.251	0.055	0.008	0.956	0.863
ADMP-043	0.889	0.186	0.085	0.430	0.708	0.209	0.032	0.010	0.952	0.662
ADMP-044	0.864	0.143	0.177	0.900	0.856	0.643	0.077	0.069	0.958	0.861
ADMP-049	0.916	0.136	0.066	0.327	0.912	0.228	0.060	0.007	0.956	0.646
TG-159	0.668	0.144	0.096	0.791	0.858	0.391	0.068	0.014	0.956	0.862
TG-160	0.671	0.126	0.067	0.746	0.852	0.382	0.071	0.011	0.957	0.768
TG-161-3	0.893	0.094	0.072	0.669	0.637	0.252	0.014	0.177	0.960	0.932
TG-163	0.626	0.144	0.121	0.639	0.873	0.311	0.070	0.010	0.956	0.863
TG-164	0.377	0.113	0.762	0.095	0.829	0.114	0.073	0.013	0.949	0.079
TG-165	0.644	0.129	0.084	0.448	0.876	0.262	0.071	0.008	0.959	0.750
MK-880	0.778	0.164	0.115	0.232	0.856	0.156	0.057	0.007	0.957	0.450
MK-881	0.979	0.378	0.648	0.821	0.844	0.590	0.043	0.104	0.961	0.799
MK-884	0.961	0.197	0.740	0.942	0.773	0.847	0.076	0.649	0.960	0.956
MK-885	0.979	0.581	0.442	0.686	0.690	0.459	0.021	0.125	0.963	0.833

The predicted metabolic pathway predominantly involves CYP3A4, as all compounds appear to be good substrates for this enzyme. In addition, CYP1A2 was expected to have a significant contribution to metabolic transformations, with most compounds showing high probabilities of being CYP1A2 substrates. However, TG-164 exhibited distinct behaviour, with a lower probability of being a CYP1A2 substrate (0.377) and a much higher probability of being a CYP2C9 substrate (0.762) compared to other BIs. Interestingly, apart from TG-164, all studied BIs seem to be potential inhibitors of CYP3A4. This is an important information for considering potential drug-drug interactions.

Table V presents the pharmacokinetic parameters relevant to elimination: clearances (CL^{IS} and CL_{int}^{IV}) and half-lives ($t_{1/2}$ *prob.*^{IS}, $t_{1/2}$ *calc.*^{IS} and $t_{1/2}^{IV}$).

CL^{IS} values ranged from 0.851 to 3.344 mL min^{-1} kg^{-1}. The highest values were reported for (+)-JQ1 (3.291 mL min^{-1} kg^{-1}) and TG-161-3 (3.344 mL min^{-1} kg^{-1}), whereas CL^{IS} for birabresib was predicted to be 1.365 mL min^{-1} kg^{-1}.

TABLE V. Clearances and half-lives of the studied compounds; Heatmap is based on an *in silico* empirical decision. Cells marked in green, yellow, or red denote excellent, medium, or poor results, respectively;[22] *CL* – total clearance; $t_{1/2}$ – half-life; CL_{int} – intrinsic clearance; *SD* – standard deviation

Compound	*In silico*-obtained results			*In vitro*-obtained results	
	CL[a] mL min^{-1} kg^{-1}	$t_{1/2}$ *prob.*[b]	$t_{1/2}$ *calc.* / h	CL_{int} / mL min^{-1} kg^{-1}	$t_{1/2} \pm SD$ / h
(+)-JQ1	3.291	0.117	4.98	51.21	0.41 ± 0.01
Birabresib	1.365	0.172	9.90	12.33	1.69 ± 0.08
ADMP-042	2.352	0.442	8.22	42.52	0.49 ± 0.03
ADMP-043	1.419	0.359	13.70	35.87	0.58 ± 0.02
ADMP-044	1.687	0.105	6.39	329.76	0.06 ± 0.00
ADMP-049	2.708	0.199	7.20	38.79	0.54 ± 0.02
TG-159	1.406	0.184	10.18	60.09	0.35 ± 0.01
TG-160	1.589	0.219	7.49	3.60	5.78 ± 0.47
TG-161-3	3.344	0.434	3.82	4.40	4.72 ± 0.59
TG-163	1.538	0.191	9.30	229.14	0.09 ± 0.01
TG-164	0.851	0.465	11.89	1.84	11.29 ± 2.41
TG-165	1.620	0.307	10.54	19.23	1.08 ± 0.03
MK-880	1.851	0.300	10.03	6.52	3.19 ± 0.13
MK-881	1.562	0.120	8.40	18.86	1.10 ± 0.11
MK-884	2.644	0.108	5.29	79.26	0.26 ± 0.03
MK-885	1.246	0.103	11.57	6.52	3.19 ± 0.13

[a]High is >15 mL min^{-1} kg^{-1}, moderate is 5–15 mL min^{-1} kg^{-1}, and low is <5 mL min^{-1} kg^{-1}. [b]The output values, ranging between 0 and 1, represent the probability that the compound has half-life >3 h

The calculated values ranged from 3.82 h (TG-161-3) to 11.89 h (TG-164). Birabresib had $t_{1/2}$ *calc.*^{IS} of 9.90 h, while it was 4.98 h for (+)-JQ1. In general, the calculated half-lives were greater than those experimentally assessed. In line with this, the Wilcoxon signed-rank test (Fig. S-3A of the Supplementary material) showed a statistically significant difference ($p < 0.001$) between half-lives obtained *in silico* and *in vitro*. The corresponding median values are 8.85 h (*IQR* 6.59–10.45 h) and 0.83 h (*IQR* 0.36–3.19 h). A bar plot with paired data (Fig. S-3B) provides a visual representation that simplifies and makes the understanding of calculated and *in vitro*-assessed half-lives more straightforward. The best agreement was observed for TG-164 (11.89 and 11.29 h, respectively), and very good agreement was noted for TG-160 and TG-161-3.

As already described, a metabolic stability assay using human liver microsomes was employed to assess intrinsic clearances (CL_{int}^{IV}) of the studied BIs.[2] The obtained results were as follows: ten compounds showed high CL_{int}^{IV}, while three compounds had moderate CL_{int}^{IV} (birabresib, MK-880, MK-885). These

molecules might be considered to have appropriate metabolic stability. By contrast, compounds showing low metabolic stability (*i.e.*, having very high CL_{int}^{IV}) had quite short $t_{1/2}^{IV}$, which ultimately makes them unsuitable for further investigation (ADMP-044 and TG-163).

Table S-I provides a detailed representation of the statistical correlations between pharmacokinetic parameters relevant to metabolism and excretion, obtained from both *in silico* and *in vitro* studies. Summarily, $t_{1/2}$ *prob.*^{IS} showed strong negative correlations with both Avg. P^{IV} and R^{IV} and a moderate negative correlation with PPB^{IV}. On the other hand, $t_{1/2}$ *calc.*^{IS} showed a moderate negative correlation with PPB^{IV}.

This study assessed the pharmacokinetic properties of BIs derived from (+)-JQ1 using *in silico* predictions from ADMETlab 2.0, which were subsequently compared with *in vitro* data. An effective *in silico* model would streamline the optimization of Bis' structures and facilitate the selection of candidates for further development, reducing the need for extensive experimental efforts. ADMETlab 2.0 was chosen for its comprehensive database and proven accuracy in predicting ADME properties.[1,20] While some discrepancies were noted between the predictions and experimental results, the tool still offered valuable insights. These differences highlight the challenges in accurately modelling pharmacokinetics computationally and emphasize the need to validate predictions with experimental data. Rather than detracting from ADMETlab 2.0's utility, the findings suggest areas for improvement in predictive models. The study focused on sixteen structurally diverse compounds, providing a detailed comparison and forming the basis for future research with larger datasets.

Absorption

Newly synthesized BIs are intended for oral administration in contemporary anticancer therapy, requiring sufficient intestinal permeability. A moderate negative correlation was observed between *HIA prob.*^{IS} (indicating the likelihood of human intestinal absorption being below 30 %) and PAMPA-obtained *in vivo* results (Avg. P^{IV} and R^{IV}). This relationship reflects the shared focus of both methods on gut wall permeability: *HIA prob.*^{IS} predicts the likelihood of absorption through the gut wall using a computational model, while PAMPA experimentally assesses passive permeability across a lipid membrane in an *in vivo* setting. The observed correlation aligns with the expectation that compounds predicted to have poor absorption by *HIA prob.*^{IS} are also less likely to exhibit high passive permeability in the PAMPA assay.

In contrast, no significant correlation was found between $F(20\%)^{IS}$ or $F(30\%)^{IS}$ and PAMPA-obtained *in vivo* results (Avg. P^{IV} and R^{IV}, Table S-I). This discrepancy arises from the distinct scope of these methods. Unlike *HIA prob.*^{IS},

which exclusively evaluates gut wall absorption, $F(20\%)^{IS}$ and $F(30\%)^{IS}$ incorporate presystemic metabolic processes, such as metabolism occurring in the gut wall or liver, to provide a broader estimate of a compound's efficiency in reaching systemic circulation. The absence of correlation with PAMPA-obtained *in vivo* results, which do not account for metabolism, highlights the differences in these methods' focus. Consequently, the moderate negative correlation between *HIA prob.*^{IS} and Avg. P^{IV} and R^{IV} reflects their mutual emphasis on gut wall permeability. In contrast, the lack of correlation between $F(20\%)^{IS}$ or $F(30\%)^{IS}$ and Avg. P^{IV} and R^{IV} underscores the influence of presystemic metabolism on these broader pharmacokinetic predictions.

No significant correlation was found between *in silico*-predicted and *in vitro*-assessed Caco-2 permeability (Fig. S-1A, Table S-I). This suggests that the *in silico* model may not fully capture the complexity of the *in vitro* conditions, which involve multiple biological processes, such as transporter interactions and efflux mechanisms, that are difficult to simulate accurately. High P_{app} A–B^{IV} values may suggest good permeability, but many BIs exhibited undesirable ER^{IV}s over 3 (Table II), indicating potential active efflux involvement that could significantly impact bioavailability. These findings highlight the limitations of relying solely on *in silico* predictions for permeability assessment, as they may overlook critical biological factors influencing drug absorption. The further refinement of predictive models, considering transporter activity and efflux mechanisms, could help improve their alignment with experimental results and enhance their use in early drug development phases.

No correlation was found between Caco-2 permeability assay obtained *Avg.* P_{app} A–B^{IV} and *MDCK perm.*^{IS}. The Caco-2 assay assesses intestinal absorption using cells derived from human colon adenocarcinoma, forming tight junctions and mimicking intestinal epithelium characteristics.[24] The alternative cell-based permeability assay employs MDCK cells. These exhibit rapid growth and differentiation, significantly shortening the duration of *in vitro* transport studies. Using MDCK cells in permeability-based assays offers an appealing substitute to Caco-2 cells, enabling the enhanced throughput and the expedited completion of transport studies for novel compounds.[25] The lack of correlation between *in vitro* assessment of Caco-2 permeability and *in silico* prediction of MDCK permeability could be due to differences in their origins, membrane composition, metabolic activity, and transporter expression.[26]

A negative correlation between *P-gp sub.*^{IS} and Avg. P^{IV} (Table S-I) is due to the physicochemical properties of P-gp substrates, which are typically larger, more polar, and have multiple hydrogen bond donors and acceptors.[27] These properties hinder passive diffusion across lipid membranes, which PAMPA measures. Thus, PAMPA assesses passive permeability, which is inversely related to P-gp substrate recognition traits.

PAMPA showed variability in Avg. P^{IV} and R^{IV} values among BIs (Table II). The highest absorption was observed for (+)-JQ1, birabresib, ADMP-044, MK--881, MK-884 and MK-885, likely due to their high log *D* values (Table S-II of the Supplementary material). Combining PAMPA and Caco-2 permeability assay results (Table II) suggests these BIs exhibit favorable permeabilities, with minimal ionization at physiological pH, except for TG-164 (Table S-II).

A negative correlation was observed between *P-gp inh.*^{IS} and ER^{IV} (Table S-I), suggesting that compounds more likely to inhibit P-gp tend to have lower ER^{IV}s. In other words, substances that inhibit P-gp-mediated efflux may lead to reduced ER^{IV}s in the Caco-2 permeability assay. This could be due to P-gp inhibitors blocking efflux activity, thereby decreasing the active drug efflux in the Caco-2 assay. Thus, higher *P-gp inh.*^{IS} values may result in lower ER^{IV}s. It can be hypothesized that the studied BIs reduce their efflux by inhibiting P-gp.

While no statistically significant correlation between *P-gp sub.*^{IS} and ER^{IV} was observed (Table S-I), a trend was noted wherein some compounds with higher *P-gp sub.*^{IS} values also exerted higher ER^{IV} values. For instance, as shown in Tables I and II, the compounds such as ADMP-042, ADMP-043, ADMP-049 and MK-880, which exhibited higher *P-gp sub.*^{IS} values (0.812, 0.992, 0.860 and 0.730, respectively), were also associated with elevated, double-digit ER^{IV} values (33.96, 11.20, 39.93 and 11.94, respectively). This observation aligns with the hypothesis that the substrates of P-gp may exhibit increased efflux, as reflected by higher ER^{IV}s. However, this relationship was not strong enough to be conclusive. Notably, phase I/II clinical trials have confirmed that new BIs are P-gp substrates but still show favourable absorption rates after oral administration.[28–32] This discordance suggests that additional factors, beyond P-gp substrate status, influence BIs' absorption.

Distribution

The distribution phase is responsible for delivering a drug to its site of action. For BIs, BBB penetration is crucial, particularly for CNS tumor treatments. Based on *BBB pen.*^{IS} values (Table III), all studied BIs, including TG-164 (despite its ionized carboxylic acid at physiological pH; Table S-II), are likely to cross the BBB, which in some cases might be desirable as birabresib has been investigated for recurrent glioblastoma multiforme.[23] A moderate positive correlation was observed between *BBB pen.*^{IS} and *Avg.* P^{IV} (Table S-I), suggesting that higher passive permeability, as assessed by PAMPA, is associated with an increased probability of BBB penetration. This correlation likely reflects the overlapping physicochemical properties required for both processes, such as optimal lipophilicity and molecular size. While passive permeability is an important determinant, other mechanisms such as active transport may also influence BBB penetration. For instance, TG-164's predicted BBB penetration, despite its ionized carboxylic acid

moiety at physiological pH, could be attributed to its amide-bound glycine group, which might facilitate LAT-1-mediated transport, similar to what is observed with levodopa.[33]

The plasma protein binding plays a critical role in drug distribution. Based on PPB^{IS} values (Table III), ten out of sixteen BIs exhibited high plasma protein binding (more than 90 %), with the highest PPB^{IS} (96.10 %) predicted for birabresib. Generally, greater lipophilicity corresponds to higher plasma protein binding, as hydrophobic compounds preferentially bind to plasma proteins for transport. This relationship was supported by strong positive correlations between PPB^{IS} and both Avg. P^{IV} and R^{IV} (Table S-I), indicating that lipophilic compounds tend to exhibit higher permeability and recovery in the PAMPA assay as well as greater protein binding. Conversely, strong and moderate negative correlations were observed between $F_u{}^{IS}$ and Avg. P^{IV}, and between $F_u{}^{IS}$ and R^{IV}, respectively, suggesting that lower unbound fractions are associated with higher permeability and recovery. This highlights the interplay between lipophilicity, protein binding, and permeability. Additional factors, such as acid-base properties and specific protein interactions, should also be considered.

A moderate positive correlation was observed between *in silico*-predicted and *in vitro*-assessed plasma protein binding values using bivariate Spearman's correlation, indicating that the *in silico* model effectively captures relative trends in plasma protein binding among the studied compounds. However, the significant differences between the two datasets, as identified by the Wilcoxon signed-rank test (Fig. S-2A), suggest some systematic discrepancies in their central tendencies. This implies that while the *in silico* model is useful for ranking compounds based on the relative plasma protein binding values, further refinement is needed to enhance its predictive accuracy for absolute values.

The volume of distribution describes the apparent distribution extent of drugs within the body.[34] ADMETlab 2.0 predictions place $V_d{}^{IS}$ values within the optimal range (0.04–20 L kg^{-1}),[22] specifically from 0.876 to 1.686 L kg^{-1}. Predicted $V_d{}^{IS}$ values exceeded the total body water (0.5–0.6 L kg^{-1}),[35] suggesting high tissue affinity. Multiplying $V_d{}^{IS}$ values by 70 kg indicates distribution between 61 and 118 L. A moderate positive correlation was observed between $V_d{}^{IS}$ and ER^{IV}, suggesting that higher efflux activity, often associated with tissue partitioning, may contribute to greater apparent distribution volumes. For example, TG-164 had a $V_d{}^{IS}$ of 0.876 L kg^{-1}, which is linked to its low log *D*, likely due to the free carboxylic acid moiety (Fig. 1). However, its high probability of BBB penetration may be attributed to active transport mechanisms, as discussed earlier, potentially involving its amide-bound glycine group facilitating LAT-1-mediated transport. ADMP--049 had the highest $V_d{}^{IS}$ (1.686 L kg^{-1}), despite its low log *D* (1.72; Table III and Table S-II). Overall, predicted $V_d{}^{IS}$ values align with those from first-in-human BI studies, which report steady-state $V_d{}^{IS}$ values of approximately 70 L.[36,37]

Metabolism and excretion

ADMETlab 2.0 predicts the probabilities of compounds being substrates or inhibitors of CYP450 isoenzymes, including CYP1A2, CYP2C9, CYP2C19, CYP2D6, and CYP3A4 (Table IV). It was predicted that CYP3A4, CYP1A2 and CYP2C19 are dominant in the metabolism of the tested BIs, and that these compounds are also likely CYP3A4 and CYP2C9 inhibitors. These insights are valuable for guiding the future research into (+)-JQ1-derived BIs. The genetic polymorphism of CYP450, particularly CYP2C19,[38] can significantly affect drug exposure and clinical outcomes, which is important as CYP2C19 is predicted to play a major role in BI metabolism (Table IV).

Selecting the optimal BI is challenging due to *in silico* results' inability to predict competition among CYP450 isoenzymes for a given compound. Nonetheless, these results align with findings that CYP3A4 is key in producing (+)-JQ1 metabolites *in vitro*.[18] Apart from its role in hepatic clearance, CYP3A4 also participates in first-pass metabolism in the gut, potentially reducing bioavailability, which could apply to the studied BIs.[39] The detailed metabolic profiling of the studied BIs might identify active metabolites; for example, molibresib forms two active metabolites via CYP3A4.[40] Evaluating BIs for CYP450 inhibition or induction is crucial for assessing drug-drug interactions. All BIs, except TG-164, were predicted to inhibit CYP2C9, CYP2C19 and CYP3A4.

Elimination of the compounds studied was evaluated through CL^{IS}, $t_{1/2}$ *prob.*^{IS} and $t_{1/2}$ *calc.*^{IS} (Table V). No correlation was found between CL^{IS} and $CL_{int}{}^{IV}$, as intrinsic clearance reflects intrinsic organ clearance independent of blood flow or binding.[41] Similarly, there was no correlation between $t_{1/2}$ *prob.*^{IS} or $t_{1/2}$ *calc.*^{IS} and $t_{1/2}{}^{IV}$, potentially due to a non-hepatic component of clearance, such as renal elimination. These discrepancies highlight that calculated half-lives might not fully capture *in vivo* dynamics. Despite these limitations, *in silico* predictions provide a basis for designing new (+)-JQ1-derived BIs.

Based on the comparative analysis of *in silico* and *in vitro* pharmacokinetic profiles, metabolic stability appears to be the most limiting factor for many of the studied BIs. Several compounds exhibited high $CL_{int}{}^{IV}$ and short $t_{1/2}{}^{IV}$ values (Table V), suggesting the rapid hepatic metabolism that could compromise systemic exposure and therapeutic efficacy. Notably, metabolism appears to be mediated by multiple CYP450 isoenzymes, especially CYP3A4, which is involved in both hepatic and intestinal first-pass metabolism, as well as CYP1A2, CYP2C9 and CYP2C19 (Table IV). This broad CYP450 involvement raises concerns not only about fast clearance but also about potential drug-drug interactions, especially in polypharmacy contexts like oncology. While some BIs demonstrated promising absorption and distribution profiles, their advancement into preclinical development may be hindered unless metabolic pathways are optimized through structural modifications or formulation strategies. Thus, metabolism – and the complexity of

CYP450-mediated biotransformation – is currently the most critical pharmacokinetic barrier for further development of these compounds.

Among the tested BIs, (+)-JQ1, ADMP-042, ADMP-049, TG-161-3 and MK--884 were predicted to have significantly higher CL^{IS} than birabresib, indicating rapid elimination (Table V). Other BIs, excluding TG-164, had CL^{IS} values comparable to birabresib. MK-880 and MK-885, alongside birabresib, showed moderate $CL_{int}{}^{IV}$ values, making them suitable for further development. Compounds with low metabolic stability, such as ADMP-044 and TG-163, exhibited high $CL_{int}{}^{IV}$ and short half-lives (3–6 min), limiting their potential for further research.[42] Conversely, highly stable compounds like TG-160, TG-161-3 and TG-164 demonstrated relatively long *in vivo* half-lives.

Taking into account the balance of absorption, distribution, metabolism, and excretion parameters, our data suggest that MK-880 and MK-885, along with the reference compound birabresib, are the most promising candidates for further investigation. These compounds exhibited moderate $CL_{int}{}^{IV}$ values (Table V), indicating acceptable metabolic stability, and had favorable plasma protein binding (Table III), adequate permeability (Tables I and II), and appropriate $V_d{}^{IS}$ values (Table III). MK-885, in particular, showed a favorable balance between *in silico* and *in vitro* data, including high passive permeability (Table II), moderate $t_{1/2}{}^{IV}$ values (Table V) and a manageable CYP450 interaction profile (Table IV). Although CYP3A4 involvement was predicted, the overall interaction profile does not suggest an unmanageable risk of drug-drug interactions. While the compounds such as TG-160 and TG-164 demonstrated prolonged $t_{1/2}{}^{IV}$ (Table V), other limitations – such as high *ER* observed for TG-160 or low permeability (Table II) and high ionization (Table S-II) of TG-164 – may reduce their immediate suitability. Therefore, from a pharmacokinetic standpoint, MK-880 and MK-885 offer the most balanced profiles, supporting their prioritization in further preclinical development.

CONCLUSIONS

This study provides a comprehensive analysis of the pharmacokinetic profiles of (+)-JQ1-derived BIs, expanding on prior work. By comparing *in silico* and *in vitro* data, we evaluated the efficacy of ADMETlab 2.0 as a screening tool for these compounds. This is the first study to explore *in silico*/*in vitro* correlations for the pharmacokinetics of newly synthesized (+)-JQ1-derived BIs. Our findings revealed a moderate negative correlation between *HIA prob.*^{IS} and PAMPA-obtained *in vivo* results (Avg. P^{IV} and R^{IV}) (Table S1), while a moderate positive correlation was observed for plasma protein binding despite statistically significant differences (Fig. S-2A). Both approaches indicated the plasma protein binding values above 90 % for most compounds (Table III). The predictions of interactions with CYP450 isoenzymes were instrumental in understanding the potential of

drug-drug interactions (Table IV). While discrepancies between CL^{IS} and $CL_{int}{}^{IV}$ (Table V) were observed, these were reasonable, given the insight $CL_{int}{}^{IV}$ offers into hepatic clearance. Overall, most compounds exhibited favorable pharmacokinetic characteristics, with MK-880 and MK-885 standing out alongside birabresib for their superior $CL_{int}{}^{IV}$ values.

We emphasized the importance of integrating *in silico* predictions with experimental data to achieve a more complete understanding of pharmacokinetic profiles. The combination of these approaches enables researchers to validate and refine predictive models, ensuring reliable data applicable to real-world drug development. Early-stage ADME screening, as demonstrated through ADMETlab 2.0, is essential for identifying promising candidates and accelerating their progression through the drug development process. However, the discrepancies between *in silico* and *in vitro* results highlight the need for further refinement of computational predictions.

SUPPLEMENTARY MATERIAL

Additional data and information are available electronically at the pages of journal website: https://www.shd-pub.org.rs/index.php/JSCS/article/view/13160, or from the corresponding author on request.

Acknowledgements. This work was supported by the Science Fund of the Republic of Serbia through Program DIASPORA (Grant No. 6463913, acronym: DeSyHPRO) and by the Ministry of Science, Technological Development, and Innovation of the Republic of Serbia through two Grant Agreements with the University of Belgrade – Faculty of Pharmacy (Nos. 451-03-65/2024-03/200161 and 451-03-66/2024-03/200161). We extend our gratitude to ALSAC and St. Jude Children's Research Hospital for their support. Our thanks go to the patients, their families, and the staff at our institution. Special thanks to the Analytical Technologies Center at the Department of Chemical Biology & Therapeutics for generating the in vitro ADME data.

ИЗВОД

КОМПАРАТИВНА АНАЛИЗА ФАРМАКОКИНЕТИЧКИХ ПРОФИЛА BET ИНХИБИТОРА: УВИД ИЗ *IN SILICO* И *IN VITRO* ПОДАТАКА

МЛАДЕН КОРАВОВИЋ[1], МИЛЕНА КОВАЧЕВИЋ[2], МАРИЈА ЈОВАНОВИЋ[2], ГОРДАНА ТАСИЋ[1], ANAND MAYASUNDARI[3], GISELE NISHIGUCHI[3], БОЈАН МАРКОВИЋ[4], ЗОРАН РАНКОВИЋ[5] и ВЛАДИМИР САВИЋ[1]

[1]Катедра за органску хемију, Универзитет у Београду – Фармацеутски факултет, Војводе Степе 450, 11221 Београд, [2]Катедра за фармакокинетику и клиничку фармацију, Универзитет у Београду – Фармацеутски факултет, Војводе Степе 450, 11221 Београд, [3]Department of Chemical Biology and Therapeutics, St. Jude Children's Research Hospital, 262 Danny Thomas Place, Memphis, TN, 38105, USA, [4]Катедра за фармацеутску хемију, Универзитет у Београду – Фармацеутски факултет, Војводе Степе 450, 11221 Београд и [5]Centre for Protein Degradation, Institute of Cancer Research, 15 Cotswold Road, Sutton, London, SM2 5NG, UK

Фармакокинетичка ограничења представљају чест узрок неуспеха у развоју лекова, што чини рану процену фармакокинетичког профила кључном за смањење финансијског ризика и усмеравање оптимизације једињења. Рачунарски алати способни да предвиђају фармакокинетичке особине представљају драгоцен ресурс за одређивање приоритета

кандидата у раним фазама откривања лекова. Ова студија пружа компаративну анализу *in silico* и *in vitro* фармакокинетичких профила BET (енг. *bromodomain and extraterminal domain*) инхибитора, са посебним освртом на шеснаест једињења изведених из (+)-JQ1 које смо претходно синтетисали. Коришћењем софтверске платформе ADMETlab 2.0, предвиђени су кључни параметри апсорпције, дистрибуције, метаболизма и екскреције (АДМЕ), који су затим упоређени са експериментално добијеним подацима. Уочена је јака корелација у вези са везивањем за плазматске протеине, док су значајна одступања примећена код вредности пермеабилности и клиренса. Анализа, такође, наглашава улогу ензима CYP3A4 као кључног фактора у метаболизму неколико BET инхибитора. Добијени резултати потврђују корисност рачунарских алата попут ADMETlab 2.0 у раној фармакокинетичкој процени, али и указују на потребу за валидацијом и додатним унапређењем предиктивних модела. Ово истраживање пружа драгоцене увиде у фармакокинетику BET инхибитора и подржава интеграцију рачунарских и експерименталних приступа у процесу откривања лекова.

(Примљено 11. децембра 2024, ревидирано 18. маја, прихваћено 15. јуна 2025)

REFERENCES

1. J. Dong, N.-N. Wang, Z.-J. Yao, L. Zhang, Y. Cheng, D. Ouyang, A.-P. Lu, D.-S. Cao, *J. Cheminformatics* **10** (2018) 29 (http://dx.doi.org/10.1186/s13321-018-0283-x)
2. M. Koravovic, A. Mayasundari, G. Tasic, F. Keramatnia, T. R. Stachowski, H. Cui, S. C. Chai, B. Jonchere, L. Yang, Y. Li, X. Fu, R. Hiltenbrand, L. Paul, V. Mishra, J. M. Klco, M. F. Roussel, W. CK. Pomerantz, M. Fischer, Z. Rankovic, V. Savic, *Eur. J. Med. Chem.* **251** (2023) 115246 (http://dx.doi.org/10.1016/j.ejmech.2023.115246)
3. C. Dhalluin, J. E. Carlson, L. Zeng, C. He, A. K. Aggarwal, M.-M. Zhou, *Nature* **399** (1999) 491 (http://dx.doi.org/10.1038/20974)
4. S.-Y. Wu, C.-M. Chiang, *J. Biol. Chem.* **282** (2007) 13141 (http://dx.doi.org/10.1074/jbc.R700001200)
5. N. Zaware, M.-M. Zhou, *Nat. Struct. Mol. Biol.* **26** (2019) 870 (http://dx.doi.org/10.1038/s41594-019-0309-8)
6. P. Filippakopoulos, S. Knapp, *Nat. Rev. Drug Discov.* **13** (2014) 337 (http://dx.doi.org/10.1038/nrd4286)
7. M. Dawson, E. M. Stein, B. J. P. Huntly, A. Karadimitris, M. Kamdar, C. Fernandez de Larrea, M. J. Dickinson, P. S.-H. Yeh, N. Daver, A. Chaidos, M. S. Tallman, R. Jiménez, T. Horner, J. Baron, J. Brennan, G. Ferron-Brady, Y. Wu, N. Karpinich, B. Kremer, A. Dhar, G. Borthakur, *Blood* **130** (2017) 1377 (http://dx.doi.org/10.1182/blood.V130.Suppl_1.1377.1377)
8. K. Ramasamy, A. Nooka, H. Quach, M. Htut, R. Popat, M. Liedtke, S. A. Tuchman, J. Laubach, C. Gasparetto, A. Chanan-Khan, M. Hertzberg, M. deMario, E. Nueesch, E. Chesne, I. Franjkovic, K. Lechner, M. Kornacker, H. J. Cho, *Blood Cancer J.* **11** (2021) 1 (http://dx.doi.org/10.1038/s41408-021-00545-w)
9. V. Moreno, M. Vieito, J. M. Sepulveda, V. Galvao, T. Hernández-Guerrero, B. Doger, O. Saavedra, C. Carlo-Stella, J.-M. Michot, A. Italiano, M. Magagnoli, C. Carpio, A. Pinto, R. Sarmiento, B. Amoroso, I. Aronchik, E. Filvaroff, B. Hanna, X. Wei, Z. Nikolova, I. Braña, *Nat. Commun.* **14** (2023) 1359 (http://dx.doi.org/10.1038/s41467-023-36976-1)
10. P. G. Aftimos, M. Oliveira, K. Punie, V. Boni, E. P. Hamilton, A. Gucalp, P. D. Shah, M. J. de Miguel, P. Sharma, L. Bauman, E. Campeau, S. Attwell, M. Snyder, K. Norek, E. Johnson, M. H. Silverman, S. Lakhotia, S. M. Domchek, J. K. Litton, M. E. Robson, *J. Clin. Oncol.* **40** (2022) 1023 (http://dx.doi.org/10.1200/JCO.2022.40.16_suppl.1023)

11. M. C. Garrett, T. Carnwath, R. Albano, Y. Zhuang, C. A. Behrmann, M. Pemberton, F. Barakat, R. Lober, M. Hoeprich, A. Paravati, M. Reed, H. Spry, D. Woo, E. O'Brien, B. VanCauwenbergh, J. Perentesis, R. Nasser, M. Medvedovic, D. R. Plas, *PLOS One* **20** (2025) e0306846 (http://dx.doi.org/10.1371/journal.pone.0306846)
12. S. A. Piha-Paul, C. L. Hann, C. A. French, S. Cousin, I. Braña, P. A. Cassier, V. Moreno, J. S. de Bono, S. D. Harward, G. Ferron-Brady, O. Barbash, A. Wyce, Y. Wu, T. Horner, M. Annan, N. J. Parr, R. K. Prinjha, C. L. Carpenter, J. Hilton, D. S. Hong, N. B. Haas, M. C. Markowski, A. Dhar, P. J. O'Dwyer, G. I. Shapiro, *JNCI Cancer Spectros.* **4** (2020) pkz093 (http://dx.doi.org/10.1093/jncics/pkz093)
13. S. Wei, Y. Sun, H. Sha, *Int. Immunopharmacol.* **29** (2015) 314 (http://dx.doi.org/10.1016/j.intimp.2015.10.036)
14. D. Shankar, G. Merchand-Reyes, N. J. Buteyn, R. Santhanam, H. Fang, K. Kumar, X. Mo, L. P. Ganesan, W. Jarjour, J. P. Butchar, S. Tridandapani, *Int. J. Mol. Sci.* **24** (2023) 7623 (http://dx.doi.org/10.3390/ijms24087623)
15. S. Kaneshita, T. Kida, M. Yoshioka, K. Nishioka, M. Raje, A. Sakashita, A. Hirano, T. Sagawa, A. Kasahara, T. Inoue, K. Fujioka, H. Nagahara, M. Wada, M. Kohno, J. W. Strovel, S. Fletcher, E. Ashihara, Y. Kawahito, *Pulm. Pharmacol. Ther.* **70** (2021) 102057 (http://dx.doi.org/10.1016/j.pupt.2021.102057)
16. S. Costantino, E. Gorica, S. A. Mohammed, M. Telesca, A. Mongelli, M. Herwig, S. Ambrosini, F. Ruschitzka, N. Hamdani, F. Paneni, *Eur. Heart J.* **45** (2024) ehae666.3756 (http://dx.doi.org/10.1093/eurheartj/ehae666.3756)
17. P. Filippakopoulos, J. Qi, S. Picaud, Y. Shen, W. B. Smith, O. Fedorov, E. M. Morse, T. Keates, T. T. Hickman, I. Felletar, M. Philpott, S. Munro, M. R. McKeown, Y. Wang, A. L. Christie, N. West, M. J. Cameron, B. Schwartz, T. D. Heightman, N. La Thangue, C. A. French, O. Wiest, A. L. Kung, S. Knapp, J. E. Bradner, *Nature* **468** (2010) 1067 (http://dx.doi.org/10.1038/nature09504)
18. F. Li, K. R. MacKenzie, P. Jain, C. Santini, D. W. Young, M. M. Matzuk, *Biol. Reprod.* **103** (2020) 427 (http://dx.doi.org/10.1093/biolre/ioaa043)
19. S. Kar, J. Leszczynski, *Expert Opin. Drug Discov.* **15** (2020) 1473 (http://dx.doi.org/10.1080/17460441.2020.1798926)
20. G. Xiong, Z. Wu, J. Yi, L. Fu, Z. Yang, C. Hsieh, M. Yin, X. Zeng, C. Wu, A. Lu, X. Chen, T. Hou, D. Cao, *Nucleic Acids Res.* **49** (2021) W5 (http://dx.doi.org/10.1093/nar/gkab255)
21. P. Schober, C. Boer, L. A. Schwarte, *Anesth. Analg.* **126** (2018) 1763 (http://dx.doi.org/10.1213/ANE.0000000000002864)
22. ADMETlab 2.0, https://admetmesh.scbdd.com/explanation/index (January 31, 2024)
23. ClinicalTrials.gov, https://clinicaltrials.gov/study/NCT02296476 (January 31, 2024)
24. P. Artursson, J. Karlsson, *Biochem. Biophys. Res. Commun.* **175** (1991) 880 (http://dx.doi.org/10.1016/0006-291X(91)91647-U)
25. W. S. Putnam, L. Pan, K. Tsutsui, L. Takahashi, L. Z. Benet, *Pharm. Res.* **19** (2002) 27 (http://dx.doi.org/10.1023/A:1013647114152)
26. D. A. Volpe, *J. Pharm. Sci.* **97** (2008) 712 (http://dx.doi.org/10.1002/jps.21010)
27. R. Didziapetris, P. Japertas, A. Avdeef, A. Petrauskas, *J. Drug Target.* **11** (2003) 391 (http://dx.doi.org/10.1080/10611860310001648248)
28. J. Lewin, J.-C. Soria, A. Stathis, J.-P. Delord, S. Peters, A. Awada, P. G. Aftimos, M. Bekradda, K. Rezai, Z. Zeng, A. Hussain, S. Perez, L. L. Siu, C. Massard, *J. Clin. Oncol.* **36** (2018) 3007 (http://dx.doi.org/10.1200/JCO.2018.78.2292)

29. R. Aggarwal, A. N. Starodub, B. D. Koh, G. Xing, A. J. Armstrong, M. A. Carducci, *Clin. Cancer Res.* **28** (2022) 3979 (http://dx.doi.org/10.1158/1078-0432.CCR-22-0175)
30. V. Moreno, J. M. Sepulveda, M. Vieito, T. Hernández-Guerrero, B. Doger, O. Saavedra, O. Ferrero, R. Sarmiento, M. Arias, J. De Alvaro, J. Di Martino, M. Zuraek, T. Sanchez-Pérez, I. Aronchik, E. H. Filvaroff, M. Lamba, B. Hanna, Z. Nikolova, I. Braña, *Ann. Oncol.* **31** (2020) 780 (http://dx.doi.org/10.1016/j.annonc.2020.03.294)
31. S. A. Piha-Paul, J. C. Sachdev, M. Barve, P. LoRusso, R. Szmulewitz, S. P. Patel, P. N. Lara Jr, X. Chen, B. Hu, K. J. Freise, D. Modi, A. Sood, J. E. Hutti, J. Wolff, B. H. O'Neil, *Clin. Cancer Res.* **25** (2019) 6309 (http://dx.doi.org/10.1158/1078-0432.CCR-19-0578)
32. K. Riddell, A. Patel, G. Collins, Y. Zhou, D. Schramek, B. E. Kremer, G. Ferron-Brady, *J. Clin. Pharmacol.* **61** (2021) 125 (http://dx.doi.org/10.1002/jcph.1711)
33. D. A. Gonzalez-Carter, Z. Y. Ong, C. M. McGilvery, I. E. Dunlop, D. T. Dexter, A. E. Porter, *Nanomed. Nanotechnol. Biol. Med.* **15** (2019) 1 (http://dx.doi.org/10.1016/j.nano.2018.08.011)
34. D. A. Smith, K. Beaumont, T. S. Maurer, L. Di, *J. Med. Chem.* **58** (2015) 5691 (http://dx.doi.org/10.1021/acs.jmedchem.5b00201)
35. John E. Hall, *Guyton and Hall Textbook of Medical Physiology*, Elsevier Health Sciences, Amsterdam, 2015 (ISBN: 9781455770052)
36. A. S. Krishnatry, A. Voelkner, A. Dhar, M. Prohn, G. Ferron-Brady, *CPT Pharmaco. Syst. Pharmacol.* **10** (2021) 709 (http://dx.doi.org/10.1002/psp4.12639)
37. E. Odore, F. Lokiec, E. Cvitkovic, M. Bekradda, P. Herait, F. Bourdel, C. Kahatt, E. Raffoux, A. Stathis, C. Thieblemont, B. Quesnel, D. Cunningham, M. E. Riveiro, K. Rezaï, *Clin. Pharmacokinet.* **55** (2016) 397 (http://dx.doi.org/10.1007/s40262-015-0327-6)
38. U. M. Zanger, M. Schwab, *Pharmacol. Ther.* **138** (2013) 103 (http://dx.doi.org/10.1016/j.pharmthera.2012.12.007)
39. M. Kato, *Drug Metab. Pharmacokinet.* **23** (2008) 87 (http://dx.doi.org/10.2133/dmpk.23.87)
40. M. A. Dawson, G. Borthakur, B. J. P. Huntly, A. Karadimitris, A. Alegre, A. Chaidos, D. T. Vogl, D. A. Pollyea, F. E. Davies, G. J. Morgan, J. L. Glass, M. Kamdar, M.-V. Mateos, N. Tovar, P. Yeh, R. G. Delgado, F. Basheer, L. Marando, P. Gallipoli, A. Wyce, A. S. Krishnatry, O. Barbash, E. Bakirtzi, G. Ferron-Brady, N. O. Karpinich, M. T. McCabe, S. W. Foley, T. Horner, A. Dhar, B. E. Kremer, M. Dickinson, *Clin. Cancer Res.* **29** (2023) 711 (http://dx.doi.org/10.1158/1078-0432.CCR-22-1284)
41. D. A. Smith, K. Beaumont, T. S. Maurer, L. Di, *J. Med. Chem.* **62** (2019) 2245 (http://dx.doi.org/10.1021/acs.jmedchem.8b01263)
42. P. D. Leeson, B. Springthorpe, *Nat. Rev. Drug Discov.* **6** (2007) 881 (http://dx.doi.org/10.1038/nrd2445).